Since January 2020 Elsevier has created a COVID-19 resource centre with free information in English and Mandarin on the novel coronavirus COVID-19. The COVID-19 resource centre is hosted on Elsevier Connect, the company's public news and information website.

Journal of Quantitative Spectroscopy & Radiative Transfer 248 (2020) 107005

Contents lists available at ScienceDirect

Journal of Quantitative Spectroscopy & Radiative Transfer

journal homepage: www.elsevier.com/locate/jqsrt

Photopolarimetrical properties of coronavirus model particles: Spike proteins number influence

Dmitry Petrov

Crimean Astrophysical Observatory (CrAO RAS), Nauchnyj, 298409, Crimea, Russian Federation

ARTICLE INFO

Article history:
Received 19 March 2020
Revised 27 March 2020
Accepted 31 March 2020
Available online 13 April 2020

Keywords:
Coronavirus
Light scattering
Intensity
Polarization
Shape matrices
Computer simulation

ABSTRACT

Coronavirus virions have spherical shape surrounded by spike proteins. The coronavirus spike proteins are very effective molecular mechanisms, which provide the coronavirus entrance to the host cell. The number of these spikes is different; it dramatically depends on external conditions and determines the degree of danger of the virus. A larger number of spike proteins makes the virus infectivity stronger.

This paper describes a mathematical model of the shape of coronavirus virions. Based on this model, the characteristics of light scattered by the coronavirus virions were calculated. It was found two main features of coronavirus model particles in the spectral region near 200 nm: a minimum of intensity and a sharp leap of the linear polarization degree. The effect of the spike protein number on the intensity and polarization properties of the scattered light was studied. It was determined that when the number of spike proteins decreases, both the intensity minimum and the position of the linear polarization leap shift to shorter wavelengths. This allows us to better evaluate the shape of the coronavirus virion, and, therefore, the infectious danger of the virus. It was shown that the shorter the wavelength of scattered light, the more reliably one can distinguish viruses from non-viruses. The developed model and the light scattering simulations based on it can be applied not only to coronaviruses, but also to other objects of a similar structure, for example, pollen.

1. Introduction

During 2002–2003, coronavirus SARS-CoV has infected 8000 people at fatality rate about 10% [1]. In 2012, more than 1700 people were infected by coronavirus MERS-CoV at fatality rate about 36% [2]. At the end of 2019 novel coronavirus disease, known as COVID-19 [3], was first reported from Wuhan City of China, and has spread around the 60 countries and territories, threatening tens of millions of people [4].

Coronaviruses cause widespread diseases, threatening human health and causing economic loss [5]. Therefore, health risks from coronaviruses are constant and long-term, with important implications for global health and economic stability. The study of the various properties of coronaviruses, in particular, the characteristics of light scattering by them, can provide new tools for their identification and study.

One of the features of the coronavirus is the presence of a certain number of spike proteins on its surface (see Fig. 1, taken from [6]), forming around the virus a kind of solar corona (due to which coronavirus got its full name). Using these spikes, the coronavirus enter into host cells. The number of these spike proteins is a fairly important characteristic of the danger of the virus. Increasing the spike proteins number per virion increases infectivity [7]. Moreover, adverse conditions such as changes in temperature and pH are leaving large areas of virion relatively free of spike proteins [8].

Thus, it is fundamentally important to evaluate the spike proteins number as an indicator of the degree of danger of a given set of virions. But many existing methods, such as real-time fluorescence-based quantitative PCR [9] allow detecting virions number only, without taking into account changes in the virion structure, such as increasing or decreasing spike proteins number. This paper describes a mathematical model that allows simulating the shape of a coronavirus with a given number of spike proteins. Also the effect of the spike proteins number on the scattered light characteristics, such as intensity and the degree of linear polarization, it is studied. This approach can be helpful in the diagnosis of coronaviruses and in assessing the effect of a variety of vaccines on their infectivity.

It should be noted, that the shape of almost all viruses is a sphere with spikes. The difference between different viruses is in the shape, size, and the number of spikes. Moreover, many types of pollen like ragweed have similar structure. So the suggested model may have broader application, not limited by coronaviruses only.

E-mail address: dvp@craocrimea.ru

https://doi.org/10.1016/j.jqsrt.2020.107005
0022-4073/

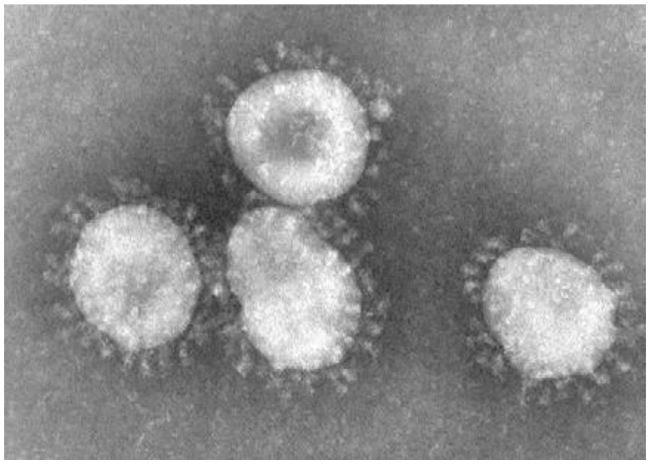

Fig. 1. Coronaviruses as seen under an electron microscope [6] (Photo courtesy of CDC/Fred Murphy).

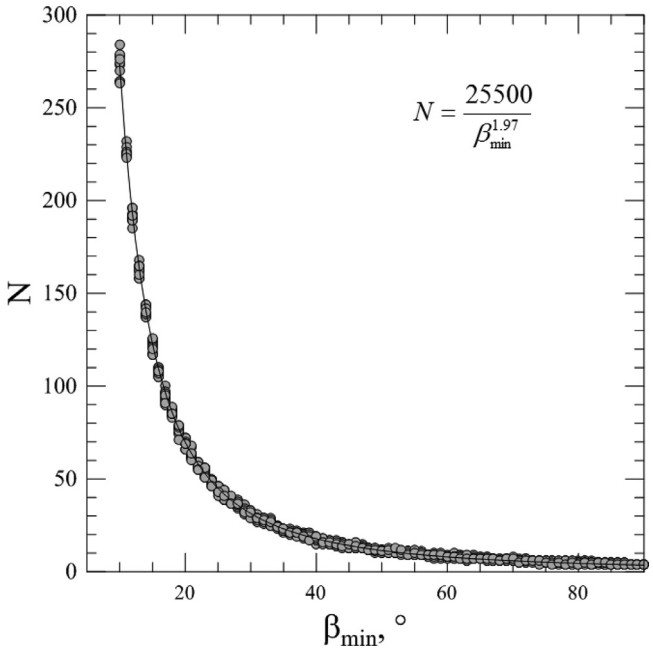

Fig. 2. The dependence of the spike proteins number on angle $\beta_{\min}$ for 10 different uses of the generation procedure (gray dots). Solid curve is the approximation by empirical Eq. (1).

2. Coronavirus virion shape simulation

As known, coronavirus virions are spherical, 120–160 nm in diameter, with an outer envelope bearing 20 nm-long club-shaped spike proteins that collectively resemble a crown or the solar corona [10]. In this paper, the following parameters of model particles are considered: virion has a diameter of 140 nm, surrounded by a set of 20 nm long spike proteins.

First of all, it is necessary to generate the distribution of spike proteins on the surface of the virion. For this, we suggest using the following generation procedure:

(1) Choose certain angle $\beta_{\min}$, which determines the minimal angle between adjacent spike proteins.
(2) Set a position of first initial spike (θ_0,φ_0). Usually we used north pole of particle (θ_0= 0, φ_0=0) for it.
(3) Generate a random position of i th spike (θ_i,φ_i) within the limits $0 \le \theta_i \le \pi$; $0 \le \varphi_i \le 2\pi$.

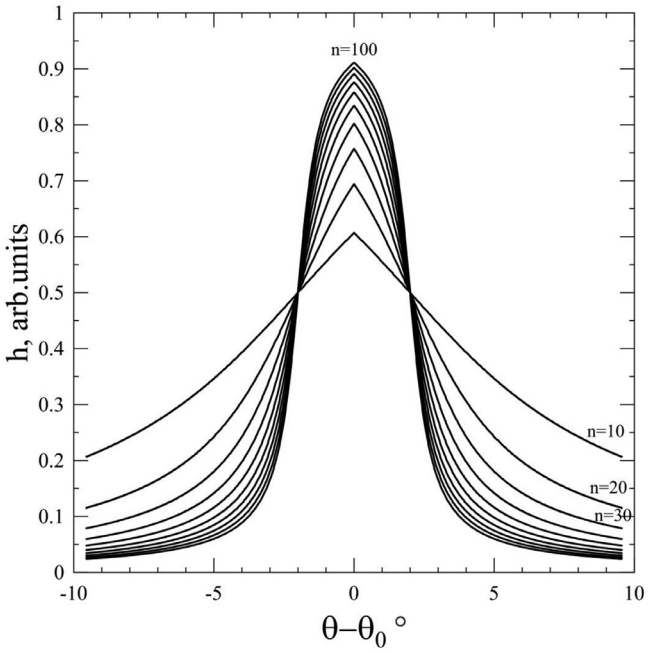

Fig. 3. Shape of individual spike proteins at different values of n.

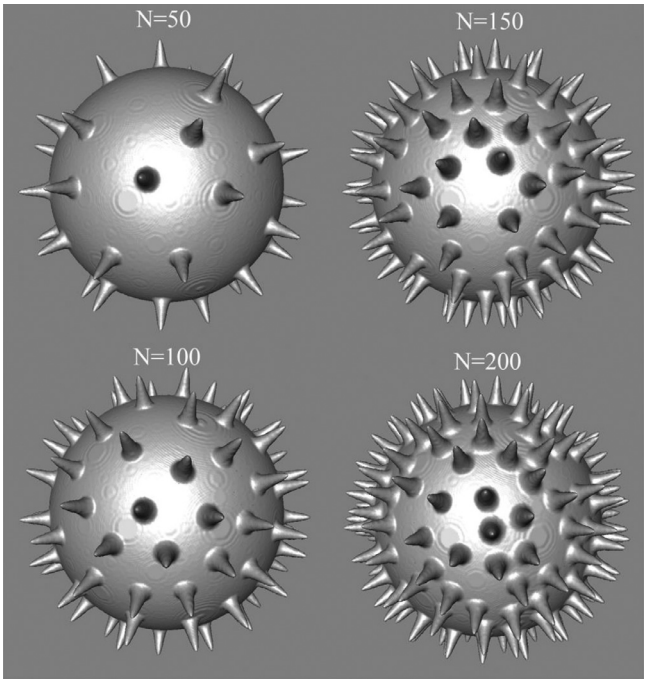

Fig. 4. An examples of coronavirus model particles with different spike proteins numbers: $N = 50$; $N = 100$; $N = 150$ and $N = 200$.

(4) Check the angular distances between i th spike and each of previous i-1 spikes.
(5) If at least one of the angles is less than $\beta_{\min}$, the position of the i th spike is regenerated.
(6) The procedure is terminated when large number (e.g. 1000) of attempts to create the i th spike is failed.
(7) As a result of procedure we obtain two arrays Θ and Φ with size N, where Θ contains set of polar angles of spikes positions, and Φ contains azimuthal angles.

It should be noted that this procedure can produce different spike proteins number N for the same minimum angle $\beta_{\min}$.

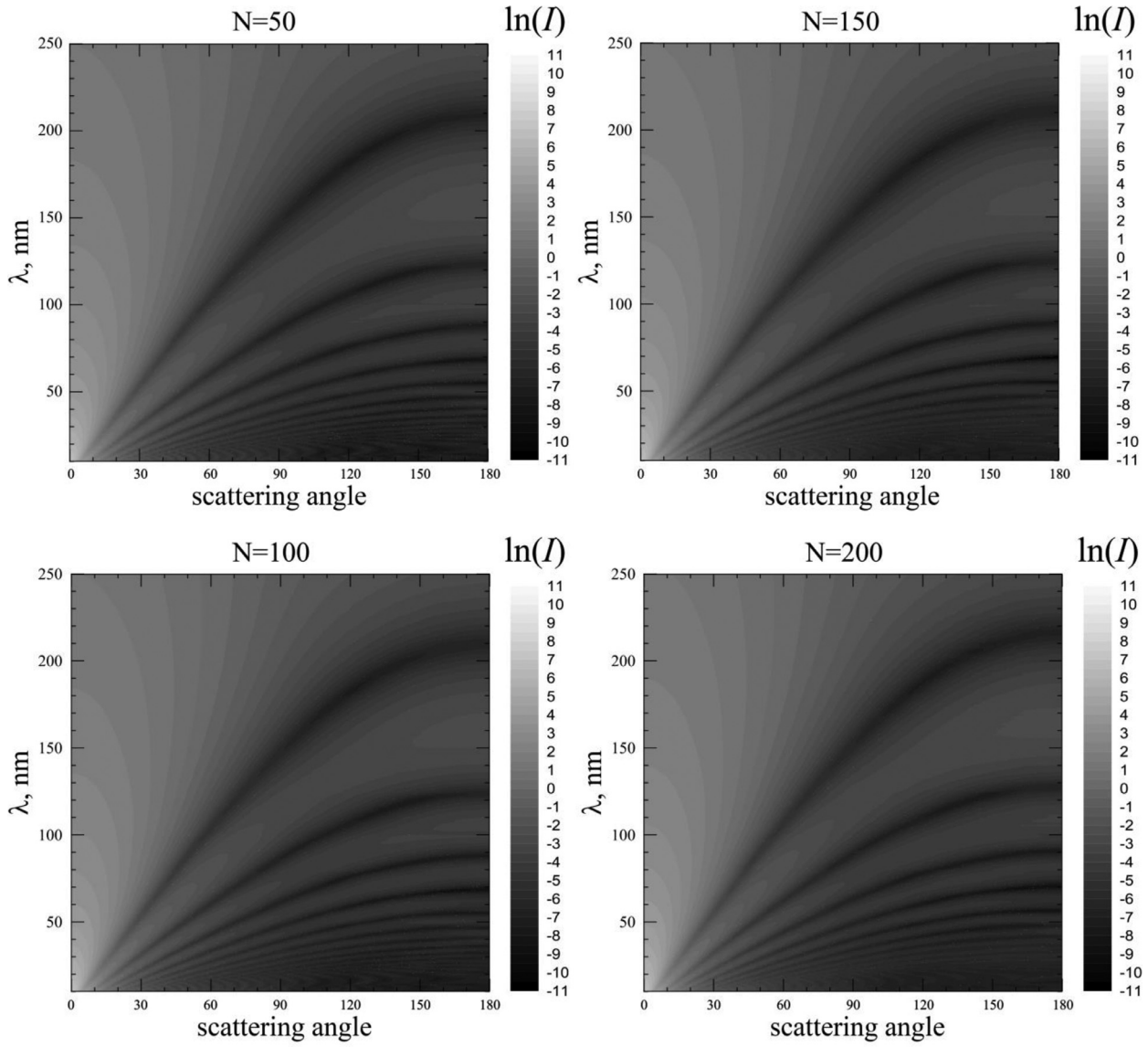

Fig. 5. Maps of intensity of light scattered by coronavirus model particles distributed over scattering angles (horizontal axis) and wavelength (vertical axis). White color corresponds to high intensity values, black – low ones. Scales are on the right side of figures. Refractive index $m_0 = 1.06$.

Fig. 2 shows the dependence of the number of spike proteins on angle $\beta_{\min}$ for 10 different uses of the above procedure (gray dots). It can be seen from the figure that the distribution of the spikes number for different angles $\beta_{\min}$ obeys a certain regularity expressed by the empirical equation (solid line in Fig. 2):

$$N = \frac{25500}{\beta_{\min}^{1.97}}, \tag{1}$$

where $\beta_{\min}$ should be expressed in degrees. This equation was obtained during searching of the best approximation of the data by function $\frac{a}{\beta_{\min}^{b}}$, where a and b were found with the help of Levenberg–Marquardt method.

Using this equation, angle $\beta_{\min}$ can be calculated for needed N value. After this, the above procedure should be repeated (as a rule, several times) in order to finally obtain the distribution of precisely N spikes on the surface of the coronavirus model particle. We used this procedure for obtain 4 sets of spike proteins: $N = 50$ ($\beta_{\min} = 23.6°$); $N = 100$ ($\beta_{\min} = 16.6°$); $N = 150$ ($\beta_{\min} = 13.5°$) and $N = 200$ ($\beta_{\min} = 11.7°$).

Spike proteins of coronavirus have a complex internal structure [11,12]. The pillows (S protein) at the end of the spikes are hard to mathematically describe. However, since these objects are much (more than order of magnitude) smaller than the wavelength of light in the spectral range studied in this paper, the effect of the specific shape of the spike protein edge seems to be rather weak. Therefore, we will try to synthesize the spike protein with a fairly smooth algebraic function. In particular, the spike can be described using the following equation:

$$h = \frac{1}{\pi}\arctan\left(\frac{2\pi n}{k} - n|\theta - \theta_0|\right) + \frac{1}{2}, \tag{2}$$

where h is the relative spike height, θ is a polar angle, θ_0 is a position of spike over polar angle (suggesting, that azimuthal angle and azimuthal position are the same $\varphi = \varphi_0$), k is the parameter, determining the width of spike, and n describes how close to the rectangle the spike shape is. Fig. 3 shows changes the spike shapes at $k = 180$ (providing half-width of spike – 2°) at different values of n. You can see, that at $n > 30$ spike becomes enough sharp.

Note, that Eq. (2) describes the 2D shape of spike, obtained by the cross section of 3-dimensional object by the meridional plane

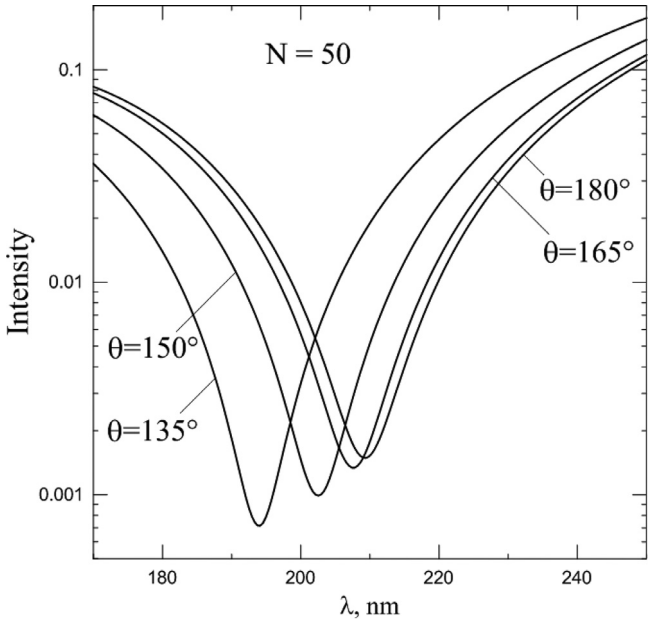

Fig. 6. Spectral dependence of intensity, scattered by coronavirus model particle with $N = 50$ spike proteins at different scattering angles. Refractive index $m_0 = 1.06$.

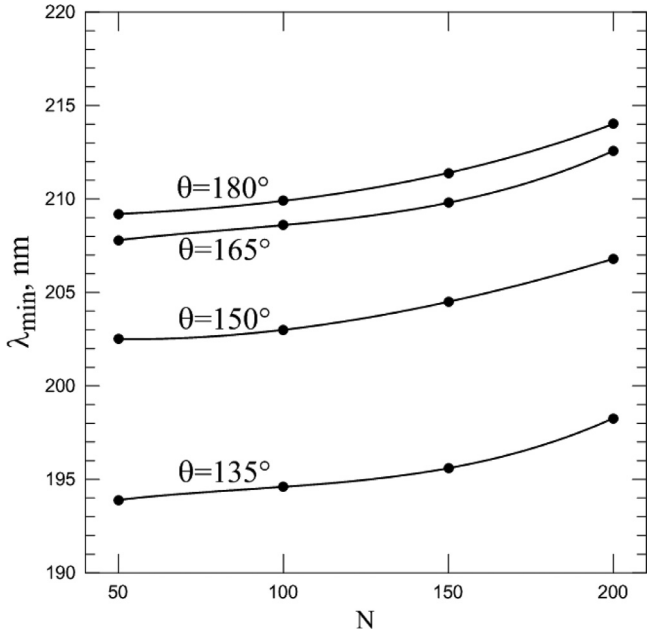

Fig. 7. Spectral position of intensity minimum at different scattering angles θ and numbers N of spike proteins (points). Lines are the approximation of each set of points by third order polynomial.

$\varphi = \varphi_0$. In the case of the transition from the two-dimensional case to the three-dimensional, we need to calculate the angle between two vectors $(\theta;\varphi)$ and $(\Theta_i;\Phi_i)$ in a spherical coordinate system. Value $\cos\beta = [\cos\theta\cos\Theta_i + \sin\theta\sin\Theta_i\cos(\varphi - \Phi_i)]$ is the cosine of angle between two vectors $(\theta;\varphi)$ and $(\Theta_i;\Phi_i)$ in spherical coordinate system. Such equation provides circular symmetry of i th spike near the direction of $(\Theta_i;\Phi_i)$.

Now we can suggest an equation, describing the shape of coronavirus model particle with N spike proteins:

$$R(\theta,\phi) = R_0 + h\left[\sum_{i=1}^{N}\left(\frac{1}{\pi}\arctan\left(\frac{2\pi n}{k} - n\cdot\arccos\left[\cos\theta\cos\Theta_i + \sin\theta\sin\Theta_i\cos(\phi-\Phi_i)\right]\right) + \frac{1}{2}\right)\right], \quad (3)$$

where R_0 and h parameters, defining the size of spherical part of virion and size of spikes, correspondingly.

In this work, we will use the following parameters: $k = 180$; $n = 50$. It should be noted, that arctan function at large values of the argument decreases rather slowly. Therefore, the closer the spikes are to each other, the higher minimal value of the function is obtained. That is why R_0 and h depend on N and was chosen so that the following conditions (determined by the size of the model particle adopted in this work — the radius of the spherical part is 70 nm, the length of the spike proteins is 20 nm) should be satisfied:

$$\begin{cases}\min[R(\theta,\phi)] = 70\\ \max[R(\theta,\phi)] = 90\end{cases}. \quad (4)$$

Fig. 4 shows examples of coronavirus model particle realizations, calculated with Eq. (3) for $N = 50$; $N = 100$; $N = 150$; $N = 200$. It will be further demonstrated how a change in the number of spike proteins affects the light scattering characteristics of such particles.

3. Light scattering computer simulation

Viruses are often suspended in liquids and may have different concentration. A most high virus concentration in eutrophic regions of world ocean is $10^{14}\ m^{-3}$ [13]. At this concentration, using simple calculations, it can be estimated that the average distance between neighboring virions is about 20 μm, while the size of the virion itself is less than 0.2 μm. So, for all viral suspension with such and lower concentrations, multiple scattering between virions is absent, and approaches that calculate scattering by an isolated particle of irregular shape can be used to calculate the scattering properties.

The T-matrix method, developed by Waterman [14] is often used to calculate the light scattering properties of individual scattering particles [15–18]. The main substance of this method is based on the expansion of the electromagnetic field incident on the particle and scattered by it in a series of vector spherical harmonics. In principle, this method can be used to study the light scattering characteristics of particles of any shape. In this work, calculations were performed by modification of the T-matrix method (the so-called *Sh*-matrices method, or the shape matrices method). This approach makes it possible to considerably simplify the calculations of arbitrary shape particles. The *Sh*-matrix technique [19,20] has been developed to study light scattering of irregular particles, comparable with wavelength, with different shapes. Moreover, analytical expressions for the calculation of *Sh*-matrix elements of arbitrary shaped particles were found [21-25]. The *Sh*-matrix elements depend only on particle morphology and are found by performing surface integrals. Size and refractive index dependences are incorporated through analytical operations on the *Sh*-matrix to produce the *T*-matrix.

In this paper we study the intensity and degree of linear polarization of scattered light on scattering angle θ, which is the angle between incident and scattered light. $\theta = 180°$ means the scattering in strong backward direction.

The particles can be characterized by the refractive index m_0. In the general case, the refractive index of the particle is complex, $m_0 = m_r + i\cdot m_i$. The question about viruses refractive index in UV is still open [26], but after studying of the four viruses investigators found, that median relative refractive index (because of virus samples are in water) in visible range is $m_0 = 1.06$ [13]. Because of it is hard to find information about the refractive index and its spectral change for viruses, calculations were carried out

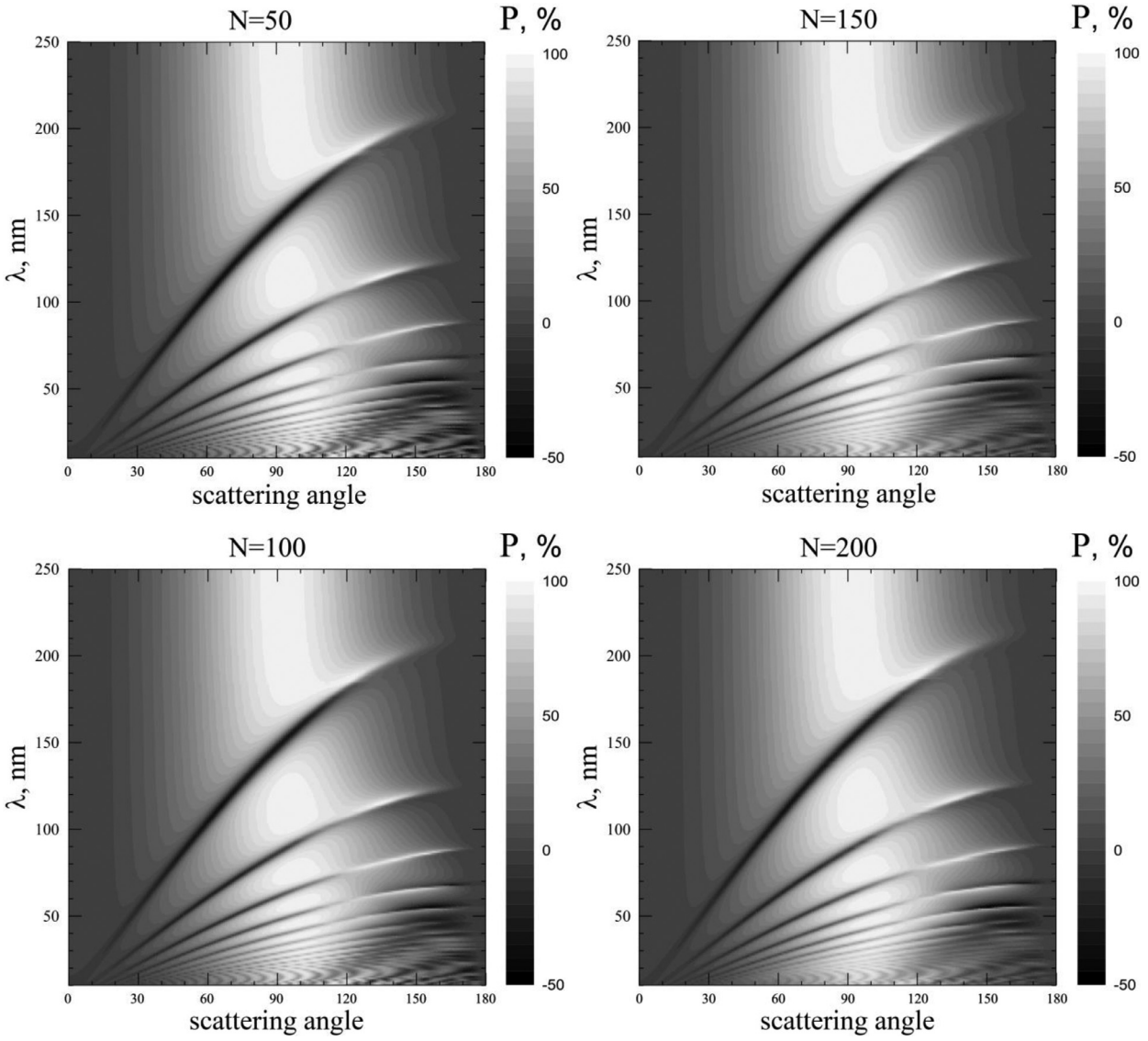

Fig. 8. Maps of degree of linear polarization distributed over scattering angles (horizontal axis) and wavelength (vertical axis). White color corresponds to high polarization values, black – low ones. Scales are on the right side of figures. Refractive index $m_0 = 1.06$.

in wavelength range from 10 to 250 nm for constant refractive index $m_0 = 1.06$. So, this paper is devoted to studying the effects of shape only. Making calculations of scattered light intensity and degree of linear polarization for coronavirus model particles, one can estimate the influence of the spike proteins number on the scattering properties of particles.

4. Results and discussion

4.1. Intensity

The results of the scattered light intensity calculations are shown on Fig. 5. On this figure you can see the maps of $\ln(I)$, where intensity depends on both scattering angle and wavelength of scattered light, at different numbers of spike proteins: $N = 50$; $N = 100$; $N = 150$ and $N = 200$. The brighter colors correspond to greater $\ln(I)$ values. Note, that calculated scattering angle dependence for each wavelength is normalized according to normalization condition [28]:

$$\frac{1}{2}\int_0^{\pi} d\theta \sin\theta \cdot I(\theta) = 1. \quad (5)$$

As can be seen from the figure, the scattering pattern has a number of noticeable features, expressed primarily in a sharp drop in the intensity of the scattered light, depending on the scattering angle and wavelength. Moreover, a distinct trend can be noted - with an increase of the spike proteins number, this minimum shifts to the region of larger wavelengths. Fig. 6 demonstrates this, showing spectral dependence of intensity at different scattering angles. It can be seen from the figure that the drop is quite strong - the intensity of the scattered light decreases by more than an order of magnitude in a sufficiently small interval of wavelengths. Therefore, wavelength λ_{min}, corresponding (at given scattering angle) to the minimum of intensity can serve as a kind of "visiting card" of the particle.

The most important question studied in this paper is how the spike proteins number affects λ_{min}? The answer is presented in Fig. 7. Here, the points correspond to the position of the minimum intensity at different scattering angles and the spike proteins number of the model particle. It can be seen from the figure that a decrease in the number of spike proteins at all scattering angles leads to a noticeable shift in the minimum of intensity toward shorter

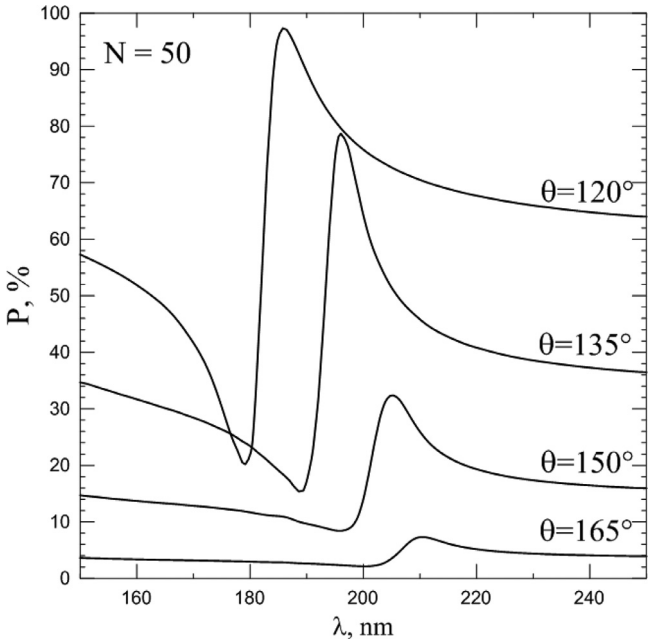

Fig. 9. Spectral dependence of linear polarization degree, scattered by coronavirus model particle with $N = 50$ spike proteins at different scattering angles. Refractive index $m_0 = 1.06$.

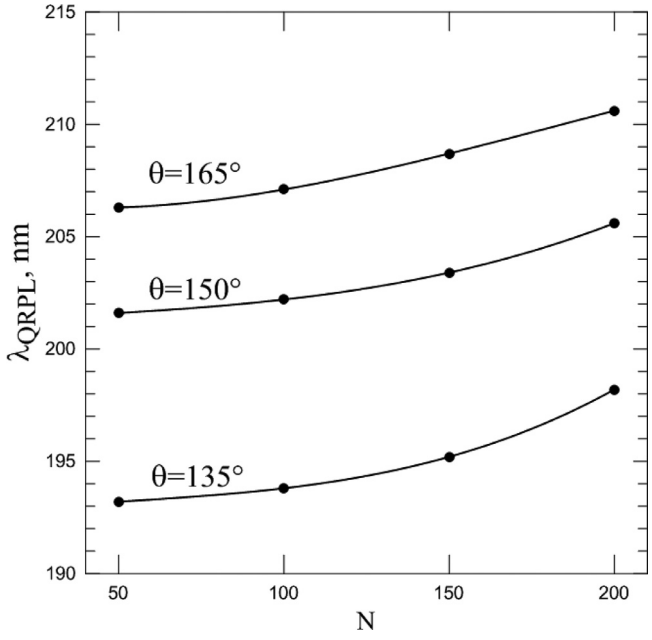

Fig. 10. Spectral position of Quasi–Rayleigh polarization leap at different scattering angles and numbers of spike proteins N (points). Lines are the approximation of each point set by third order polynomial.

wavelengths. Those, decrease in the infectivity danger of the virus is accompanied by a decreasing of λ_{min}.

4.2. Polarization

The linear polarization of scattered light by is characterized by the following equation:

$$P = \frac{I_{\perp} - I_{||}}{I_{\perp} + I_{||}} \tag{6}$$

where $I_{\perp}$ and $I_{||}$ are the intensity of perpendicular and parallel components of scattered light with respect to the scattering plane.

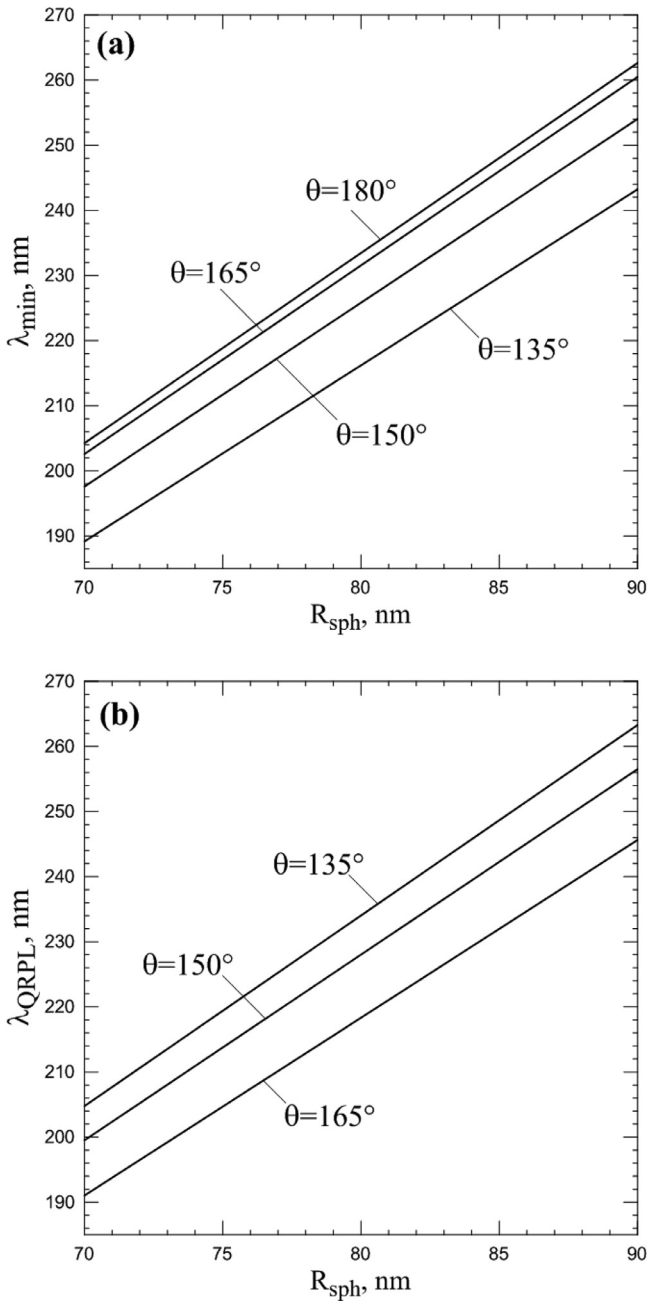

Fig. 11. Spectral position of intensity minimum (upper panel) and Quasi–Rayleigh polarization leap (lower panel) at different scattering angles and numbers for smooth sphere with radius R_{sph}. Refractive index $m_0 = 1.06$.

Fig. 8 shows maps of the degree of linear polarization of coronavirus model particles for different values of spike proteins. The X axis corresponds to the scattering angle values, and the Y axis - to the wavelengths. The degree of linear polarization is shown by different shades of gray: darker shades correspond to smaller polarization. An interesting polarization feature is observed in the spectral region of about 200 nm. If we consider it in more detail (see Fig. 9), it becomes clear that it consists in a very sharp jump in the degree of linear polarization with increasing wavelength. This feature is clearly manifested in spherical particles and is called the Quasi–Rayleigh polarization leap (QRPL) [29]. QRPL can occur even at refractive indices close to 1, and depends on the scattering angle, on the size, on the refractive index, and on the shape of the scattering particle [30].

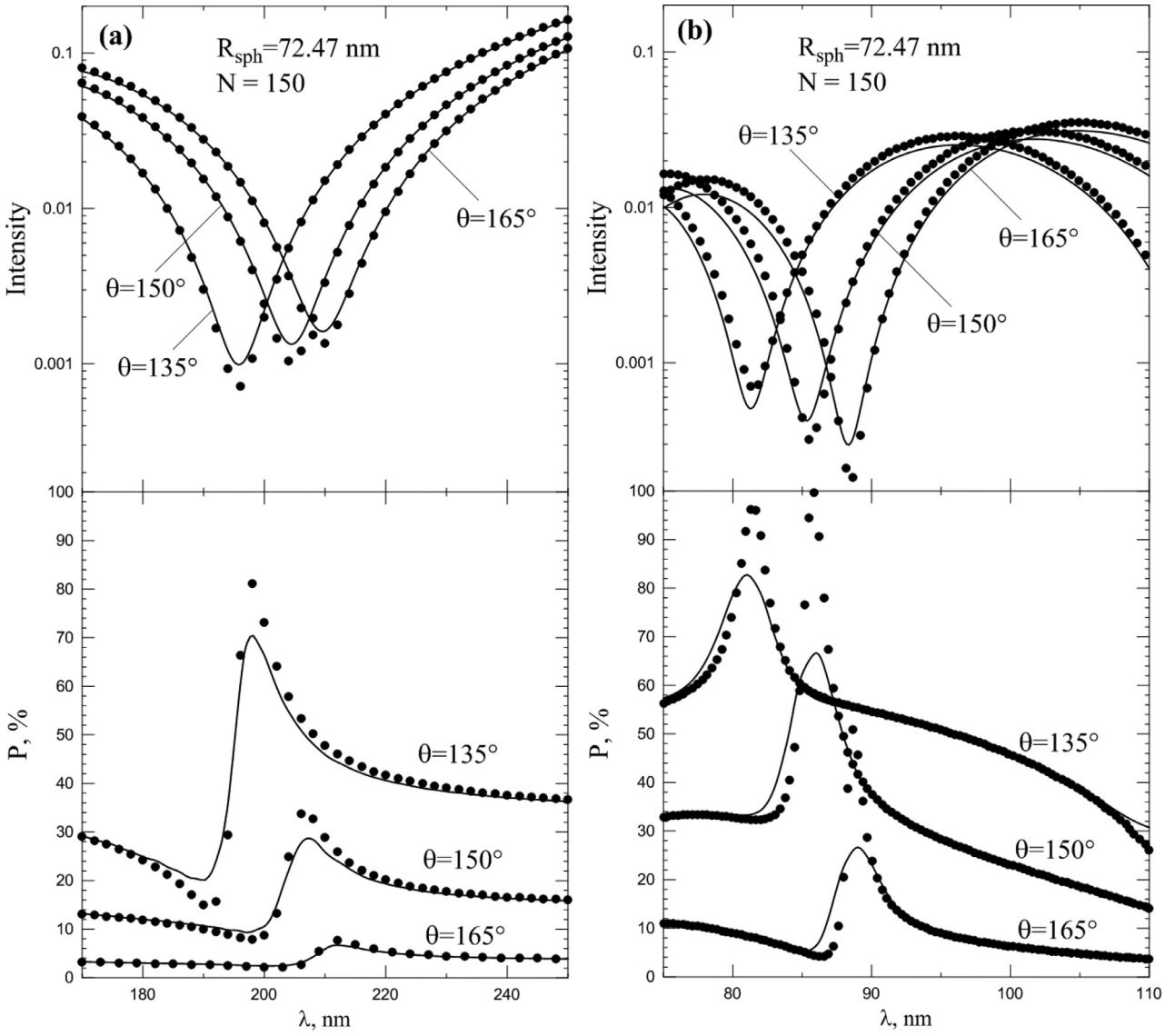

Fig. 12. Spectral dependence (λ = 170…250 nm (a); λ = 75…110 nm (b)) of intensity (upper panels) and linear polarization degree (lower panels), scattered by coronavirus model particle with N = 150 spike proteins (lines) at different scattering angles. Points correspond to intensity and polarization of smooth sphere with R_{sph} = 72.47 nm. Refractive index m_0 = 1.06.

This phenomenon can be characterized by wavelength λ_{QRPL} at which the rate of polarization change (i.e., the value of the derivative $\frac{dP}{d\lambda}$) is maximal. In this case, we see that the spike proteins number also affects the position of the QRPL. As can be seen from Fig. 10, the QRPL exhibits a behavior similar in intensity to a change in the spike proteins number. The smaller N, and the less dangerous the virus, the shorter the wavelengths corresponds to QRPL. It should be noted that λ_{min} and λ_{QRPL} differ in their values; therefore, they can be used by researchers as two independent sources of information about the spike proteins number.

4.3. Comparison with smooth spheres

The scattering patterns shown on Figs. 5 and 8 are quantitatively similar to the Mie scattering pattern. Both intensity minimum and polarization leap are representative in Mie scattering too. This is not surprising since the particles are based on a sphere, and the refractive index is closed to unity. The interesting question arises: can the scattering features described above be reproduced by a smooth sphere of a specific size? To study this issue, the calculations of λ_{min} (Fig. 11a) and λ_{QRPL} (Fig. 11b) were carried out for smooth spheres with range of sphere radii R_{sph} from 70 to 90 nm. As can be seen, λ_{min} and λ_{QRPL}Quasilinearly depend on R_{sph}. Consequently, it is formally possible to choose a radius of the sphere that reproduces scattering features described above.

Fig. 12a shows the results of Mie calculation for smooth spherical particles of radius R_{sph} = 72.47 nm (points), whose size provides the best approximation of scattering pattern of coronavirus model particle with N = 150 spike proteins (lines) in spectral region λ = 170…250 nm. Upper part shows the intensity, lower-degree of polarization. As can be seen, smooth spheres provide quantitatively different data, than model particles. This difference is most noticeable in the case of linear polarization degree, where the differences may reach about 10% on absolute value. This feature can be used for distinguishing viruses from non-viruses based on their light scattering in the cases when the size of the objects is not accurately determined.

Fig. 12b shows the same as Fig. 12a, but for spectral region $\lambda = 75...110$ nm. The figure clearly shows that subsequent resonances in light scattering make the difference with smooth spheres more noticeable. It's because spikes begin to exhibit non-Rayleigh scattering at wavelength decreasing, which means more and more depolarize light. In principle, depolarization of light scattered by model particles is associated with light scattering between the spikes, i.e. with multiple scattering, which always depolarizes light. Moreover, this multiple scattering will be more pronounced for spikes comparable to the wavelength than for those that are much smaller than the wavelength. Those, the shorter the wavelength at which observations are carried out, the more reliably one can distinguish viruses from non-viruses.

5. Concluding remarks

We suggest a method to estimate the spike proteins number of the coronavirus virion. In the region of about 200 nm, two main features are observed for coronavirus model particles-a minimum of intensity and sharp leap of the linear polarization degree. With a decrease in the number of spike proteins (and, consequently, a decrease in the infectious danger of the virus), both of these features exhibit a characteristic tendency to shift to shorter wavelengths. Therefore, this method allows you to evaluate the comparative effect of various external conditions (for example, various vaccines) on the infectious danger of the virus.

There is a fairly wide variety of different coronaviruses. Some publications note that certain varieties of coronaviruses may have the same shape, but somewhat different sizes [31]. So, the main problem is how to differentiate the signal measured from a completely different particle in the same size range, especially when noise is taken into consideration. But, since light scattering depends on the ratio of the particle size to the wavelength (size parameter), all features of model particle scattering, considered in this paper, will appear for particles having other size, manifesting themselves at shorter wavelengths for smaller particles and at larger wavelengths for greater ones. Despite noise and other particles presence, it is possible to detect a tendency to change of λ_{min} and λ_{QRPL} and the direction of their changes.

In this work, author tried to limit himself to considering only those scattering features that are in the near ultraviolet region $>$190 nm. Currently, there are many instruments that allow photometric and polarimetric measurements of biological samples in this spectral range (for example, the spectropolarimeter Jasco J-810 [27]). In addition, there is a Mueller matrix polarimeter, which can carry out measurements at incident angle of light from 0° to near 180° [32]. However, the simulation carried out in the paper shows that far ultraviolet photopolarimeters are required for a more reliable distinction between viruses of non-viruses.

At shorter wavelengths, as can be seen from Figs. 5 and 8, many other features are observed. In the case of using the appropriate measuring technique, the mathematical model suggested in this paper for describing the shape of coronavirus model particles and the calculation of its photopolarimetrical properties can be very useful.

This simulation is applicable not only to coronaviruses, but also to other objects of a similar structure, for example, pollen. Pollen particles are much larger, and therefore is none problem with their measurements right now. In the future, we will certainly apply this model to pollen samples.

Declaration of Competing Interest

The authors declare that they have no known competing financial interests or personal relationships that could have appeared to influence the work reported in this paper.

Acknowledgments

The author is grateful to Olga Pernatskaya, head of the House Museum of Anton Chekhov in Yalta, for wisdom comments and useful advices.

References

[1] Rota PA, Oberste MS, Monroe SS, Nix WA, Campagnoli R, Icenogle JP, Peñaranda S, Bankamp B, Maher K, Chen MH, Tong S, Tamin A, Lowe L, Frace M, DeRisi JL, Chen Q, Wang D, Erdman DD, Peret TC, Burns C, Ksiazek TG, Rollin PE, Sanchez A, Liffick S, Holloway B, Limor J, McCaustland K, Olsen-Rasmussen M, Fouchier R, Günther S, Osterhaus AD, Drosten C, Pallansch MA, Anderson LJ, Bellini WJ. Characterization of a novel coronavirus associated with severe acute respiratory syndrome. Science 2003;300(5624):1394–9. https://doi.org/10.1126/science.1085952.

[2] de Groot RJ, Baker SC, Baric RS, Brown CS, Drosten C, Enjuanes L, Fouchier RA, Galiano M, Gorbalenya AE, Memish ZA, Perlman S, Poon LL, Snijder EJ, Stephens GM, Woo PC, Zaki AM, Zambon M, Ziebuhr J. Middle east respiratory syndrome coronavirus (MERS-CoV): announcement of the coronavirus study group. J Virol 2013;87(14):7790–2. https://doi.org/10.1128/JVI.01244-13.

[3] Heymann DL, Shindo N. COVID-19: what is next for public health? Lancet 2020;395(10224):P542–5. https://doi.org/10.1016/S0140-6736(20)30374-3.

[4] Hu Z, Yang Z, Li Q, Zhang A, Huang Y. Infodemiological study on COVID-19 epidemic and COVID-19 infodemic. Preprints 2020 2020020380. doi:10.20944/preprints202002.0380.v2.

[5] Duan H, Wang S, Yang C. Coronavirus-limit the short-term economic damage. Nature 2020;578(7796):515. https://doi.org/10.1038/d41586-020-00522-6.

[6] Editor(s) Korsman Stephen NJ, van Zyl Gert U, Nutt Louise, Andersson Monique I, Preiser Wolfgang. Human coronaviruses. In: Korsman Stephen NJ, van Zyl Gert U, Nutt Louise, Andersson Monique I, Preiser Wolfgang, editors. Virology Churchill Livingstone; 2012. p. 94–5.

[7] Schiller J, Chackerian B. Why HIV virions have low numbers of envelope spikes: implications for vaccine development. PLoS Pathog 2014;10(8):e1004254. https://doi.org/10.1371/journal.ppat.1004254.

[8] Sturman LS, Ricard CS, Holmes KV. Conformational change of the coronavirus peplomer glycoprotein at pH 8.0 and 37 °C correlates with virus aggregation and virus-induced cell fusion. J Virol 1990;64(6):3042–50.

[9] SA Bustin. Real-time, fluorescence-based quantitative PCR: a snapshot of current procedures and preferences. Expert Rev Mol Diagn 2005;5(4):493–8. doi:10.1586/14737159.5.4.493.

[10] Pellett PE, Mitra S, Holland TC. Chapter 2 - Basics of Virology; Handbook of Clinical Neurology, 123. Elsevier; 2014. p. 45–66.

[11] Structure Li F. Function, and evolution of coronavirus spike proteins. Annu Rev Virol 2016;3:237–61. https://doi.org/10.1146/annurev-virology-110615-042301.

[12] Wrapp D, Wang N, Corbett KS, Goldsmith JA, Ch-L Hsieh, Abiona O, Graham BS, Mclellan JS. Cryo-EM structure of the 2019-nCoV spike in the prefusion conformation. Science 2020 eabb2507. doi:10.1126/science.abb2507.

[13] Balch WM, Vaughn J, Novotny J, Drapeau DT, Vaillancourt R, Lapierre J, Ashe A. Light scattering by viral suspensions. Limnol Oceanogr 2000;45(2):492–8. https://doi.org/10.4319/lo.2000.45.2.0492.

[14] Waterman PC. Numerical solution of electromagnetic scattering problems. In: Computer Techniques for Electromagnetics. Pergamon Press; 1973. p. 97–157.

[15] Mishchenko MI, Travis LD, Mackowski DW. T-matrix computations of light scattering by nonspherical particles: a review. J Quant Spectrosc Radiat Transfer 1996;55:535–75. doi:10.1016/0022-4073(96)00002-7.

[16] Mishchenko MI, Travis LD, Lacis AA. Scattering, Absorption, and Emission of Light by Small Particles. Cambridge University Press; 2002.

[17] Mishchenko MI. Electromagnetic scattering by nonspherical particles: a tutorial review. J Quant Spectrosc Radiat Transfer 2009;110:808–32. doi:10.1016/j.jqsrt.2008.12.005.

[18] Petrov D, Synelnyk E, Yu Shkuratov, Videen G. The *T*-matrix technique for calculations of scattering properties of ensembles of randomly oriented particles with different size. J Quant Spectrosc Radiat Transfer 2006;102:85–110. doi:10.1016/j.jqsrt.2006.02.077.

[19] Petrov D, Yu Shkuratov, Videen G. Electromagnetic wave scattering from particles of arbitrary shapes. J Quant Spectrosc Radiat Transfer 2011;112:1636–45. doi:10.1016/j.jqsrt.2011.01.036.

[20] Petrov D, Yu Shkuratov, Videen G. Light scattering by arbitrary shaped particles with rough surfaces: *sh*-matrices approach. J Quant Spectrosc Radiat Transfer 2012;113:2406–18. doi:10.1016/j.jqsrt.2012.04.016.

[21] Petrov D, YuG Shkuratov, Videen G. Sh-matrices method as applied to scattering by particles with layered structure. J Quant Spectrosc Radiat Transfer 2007;106(1–3):437–54.

[22] Petrov D, YuG Shkuratov, Videen G. Influence of corrugation on light-scattering properties of capsule and finite-cylinder particles: analytic solution using *sh*-matrices. J Quant Spectrosc Radiat Transfer 2008;109(4):650–69.

[23] Petrov D, YuG Shkuratov, Videen G. Light scattering by a finite cylinder containing a spherical cavity using sh-matrices. Opt Commun 2009;282(2):156–66.

[24] Petrov D, YuG Shkuratov, Videen G. An analytical solution to the light scattering from cube-like particles using sh-matrices. J Quant Spectrosc Radiat Transfer 2010;111(3):474–82.

[25] Petrov D, Shkuratov Y, Videen G. Electromagnetic wave scattering from cuboid-like particles using sh-matrices. J Quant Spectrosc Radiat Transfer 2011;112(2):155–62.
[26] Kowalski W. UVGI disinfection theory. Ultraviolet Germicidal Irradiation Handbook. Berlin, Heidelberg: Springer; 2009.
[27] Kelly SM, Jess TJ, Price NC. How to study proteins by circular dichroism. Biochim Biophys Acta 2005;1751:119–39.
[28] Mishchenko MI, Travis LD. Capabilities and limitations of a current fortran implementation of the t-matrix method for randomly oriented, rotationally symmetric scatterers. J Quant Spectrosc Radiat Transfer 1998;60(3):309–24.
[29] Petrov DV, Zhuzhulina EA. Quasi-rayleigh polarization leap of monodisperse spherical particle as a tool to detect particle radius. J Quant Spectrosc Radiat Transfer 2020;242:106806.
[30] Petrov DV, Zhuzhulina EA. Spectral dependence of quasi-Rayleigh polarization leap of nonspherical particles: polystyrene beads application. Spectroscopy and Spectral Analysis 2020 (in press).
[31] Siegel R.D. 201 - Classification of human viruses. Principles and Practice of Pediatric Infectious Diseases (Fourth Edition), 2012, 1015–9.e1.
[32] Nouri SA, Gregory DA, Fuller K. Development of an angle-scanning spectropolarimeter: preliminary results. J Quant Spectrosc Radiat Transfer 2018;206:342–54.